applied sciences

MDPI

Article

Hydrochemical Processes and Isotopic Study of Geothermal Springs within Soutpansberg, Limpopo Province, South Africa

Olatunde Samod Durowoju [1,*], Mike Butler [2], Georges-Ivo Ekosse Ekosse [3] and John Ogony Odiyo [1]

1 Department of Hydrology and Water Resources, University of Venda, Private Bag X5050, Thohoyandou 0950, South Africa; john.odiyo@univen.ac.za
2 iThemba Labs, Environmental isotope laboratory, Private bag 11, Wits, Johannesburg 2050, South Africa; butler@tlabs.ac.za
3 Directorate of Research and Innovation, University of Venda, Private Bag X5050, Thohoyandou 0950, South Africa; Georges-Ivo.Ekosse@univen.ac.za
* Correspondence: durotunde@gmail.com; Tel.: +27-780-642-299

Received: 23 January 2019; Accepted: 27 February 2019; Published: 24 April 2019

Abstract: Geothermal springs and boreholes within the Soutpansberg Group were sampled and analysed for their major ion chemistry and stable isotope compositions in order to ascertain the possible sources and geochemical processes of the waters. The temperature of the geothermal springs ranges from 41 °C to 49 °C (thermal/hot waters) and 53 °C to 69 °C (scalding/hyperthermal waters). The major water types are Na-Cl and Na-HCO_3, which are typical of marine and deep groundwaters influenced by ion-exchange processes. The hydrochemical parameters suggest that thermal gradient, carbonate weathering, mineral dissolution, ion exchange, and evaporation are the main geochemical processes controlling the geothermal springs. The $\delta^{18}O$ and $\delta^{2}H$ values vary from −5.82‰ to −4.82‰ for $\delta^{18}O$ and −33.5‰ to −24.6‰ for $\delta^{2}H$ for all the geothermal spring water. The isotopic ranges of the groundwater are relatively smaller and more depleted than those of rainwater ($\delta^{2}H$ = −9.8‰ and $\delta^{18}O$ = −2.7‰). The $\delta^{2}H$ and $\delta^{18}O$ signatures reveal a significant infiltration before evaporation. The $\delta^{2}H$ and $\delta^{18}O$ values further confirm that the waters are of meteoric origin, which implies that modern rainfall is the fundamental component of recharge derived from the infiltration of local precipitation with significant contribution of another type of water in the deeper part of the aquifer. These results provide further insight into this basement aquifer, which is a vital resource for the region.

Keywords: geochemical process; geothermal springs; meteoric origin; Soutpansberg; stable isotopes; water type

1. Introduction

Geothermal springs are geological phenomena that occur in all parts of the world. They could be of volcanic or meteoric origin [1,2] with uses ranging from power generation, industrial processing, agriculture, aquaculture, bottled water, the extraction of rare elements, and the use of thermophilic bacteria for industrial purposes, among others [1]. The socio-economic importance of geothermal springs has fluctuated over time, but over the past few decades, there has been an unprecedented resurgence of interest in this resource mainly due to a diversification in the application of the waters [1–3].

South Africa is richly endowed with geothermal springs with about 30% of these springs found in Limpopo Province [1]. The geothermal springs in the Province were classified according to the residing mountain—Waterberg Group, Soutpansberg Group, and Drakensberg Group [2]. For this study,

the geothermal springs within the Soutpansberg Group (Basin and Karoo Trough) were investigated (Figure 1). These geothermal springs are associated with faults and impermeable dykes and are assumed to be of meteoric origin [1,3]. The optimal utilisation of geothermal springs is generally dependent upon their physical and chemical properties, and additionally, the geological formation found at the depth of origin. Individuals have utilised geothermal spring waters for different purposes for many years, ranging from bathing, therapeutic, religious, hygienic, and social purposes in several nations in the world [4,5].

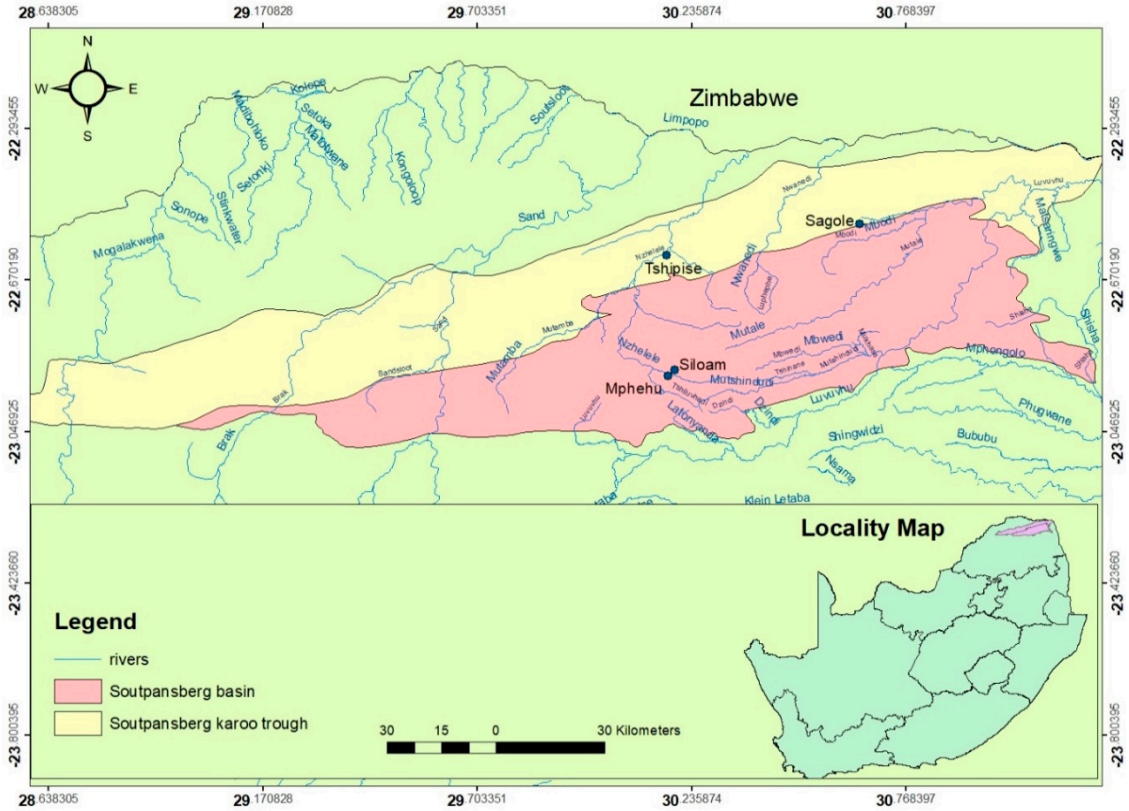

Figure 1. Hydrogeological map with Soutpansberg basin/Soutpansberg Karoo Trough located in the northern part of South Africa, showing the locations of geothermal springs.

Gonfiantini [6] reported that environmental hydrogen and oxygen isotopes are ideal tracers of water systems since they are incorporated in the water molecules and therefore their behaviour and variations reflect the origin, the hydrological and geochemical processes that affect natural water bodies. Environmental isotopes with hydrochemical data are viable tools for understanding groundwater dynamics within the Soutpansberg basin because they provide critical information about sources of groundwater recharge, timing of recharge, water-rock interaction along flow paths, and mixing of distinct groundwater bodies [7]. This is despite the fact that groundwater is greatly affected by the geochemical processes occurring within the groundwater and interaction with the aquifer material leading to seasonal and spatial variations in the groundwater chemistry [8]. Hence, the geochemical characteristics of groundwater depend on the different geochemical processes and chemistry of water at the recharge area [9].

Some studies have been carried out on Limpopo geothermal springs ranging from hydrogeology, water quality, impacts on the surrounding soils and vegetation [10–15], and recently, Durowoju et al. [16–18]. None of these studies elucidated the isotopic signatures in relation to the hydrochemical parameters of the geothermal springs. There is a need to understand the groundwater system and chemical processes governing the resources such as sources, water types, and groundwater recharge, among others. The knowledge of the groundwater system and chemical processes will help to

improve on the sustainability and development of the water resources within the locality. Already, some of the geothermal springs in Limpopo Province experience reduction in their yield and even dry up. For example, the hottest geothermal spring in the country—found at Siloam village—has dried up. Therefore, to avert these occurrences in the future, such studies have to be undertaken to improve knowledge of the hydrogeological systems of the geothermal springs for effective sustainability of the resources.

In order to increase the understanding of the geothermal spring systems, this study focuses on delineation of geothermal systems by means of environmental stable isotope (^{2}H and ^{18}O) and hydrochemical parameters in relation to geology of the area. Hence, this study is aimed at understanding the geochemical processes and possible sources of these geothermal springs/boreholes within Soutpansberg. The application of all these different methods to the hydrochemical and isotope data allowed us to characterise the mechanisms of mineralisation of groundwater. Such knowledge is important, particularly in providing relevant management options towards achieving the optimum integrated water resources management. This will further result in the maximum exploration of the potential of the geothermal spring water to be used for the benefits of the local communities (for domestic and recreational purposes) in the future.

2. Study Area

Mphephu and Siloam, Sagole, and Tshipise springs are located in Makhado, Mutale, and Musina municipalities, respectively, in Vhembe District, Limpopo Province of South Africa (Figure 1). The study areas fall under quaternary catchments of the Nzhelele River catchment (within the Soutpansberg Group), which is in the northern region of Limpopo Province, South Africa [19]. The coordinates, altitudes, and geological structures associated with the springs are presented in Table 1.

Table 1. Geographical coordinates, altitudes, and geological structures associated with springs.

Sampling Site	Sites Coordinates	Altitude (m)	Surface Geology and Geological Structures
Mphephu	30°10′35.582″ E 22°54′26.280″ S	890	Quartzite and Sandstone Reverse fault between Waterberg Group quartzite and Dominion Reef lava
Sagole	30°39′07.128″ E 22°31′49.440″ S	450	Mudstone, shale, subordinate micaceous sandstone, carbonaceous shale, siltstone, micaceous sandstone. Mikambeni Formation and Madzaringwe Formation, Karoo Supergroup
Siloam	30°10′59.988″ E 22°52′58.800″ S	835	Basalt, minor tuff Sibasa Formation, Soutpansberg Group
Tshipise	30°10′20.712″ E 22°36′31.320″ S	520	Basalt, minor andesite, cream-coloured sandstone, dolerite sills, and dykes Intersection of 2 post-Permian faults in upper Karoo

According to the Geological Survey: 1:250 000 Messina; Kent [1,20]; Olivier et al. [3].

Groundwater occurrence is mainly related to secondary hydrogeological features; that is, fault and joints, which present preferential pathways and thus enhance the potential for groundwater flow in the region. The geology determines the extent to which the reaction with the host rock proceeds depending on the chemical composition of the rock and the rate at which water passes through the rock.

2.1. Climate of the Study Area

The studied areas were categorised under the hot semi-arid region [21]. It receives much of its rainfall during summer (November to February), as the area is within the northward and southward oscillation of the inter-tropical convergence zone (ITCZ) and is associated with southerly monsoon

winds. The areas were characterised by high-temperature variations in different seasons of the year with temperatures in winter ranging from 16 °C to 22 °C, and in summer from 22 °C to 40 °C (Figure 2) [22]. The mean annual rainfall of Nzhelele ranges from 350–400 mm per annum [19]. More than 80% of the rainfall occurs in the summer, and only about 20% occurs in the winter [23].

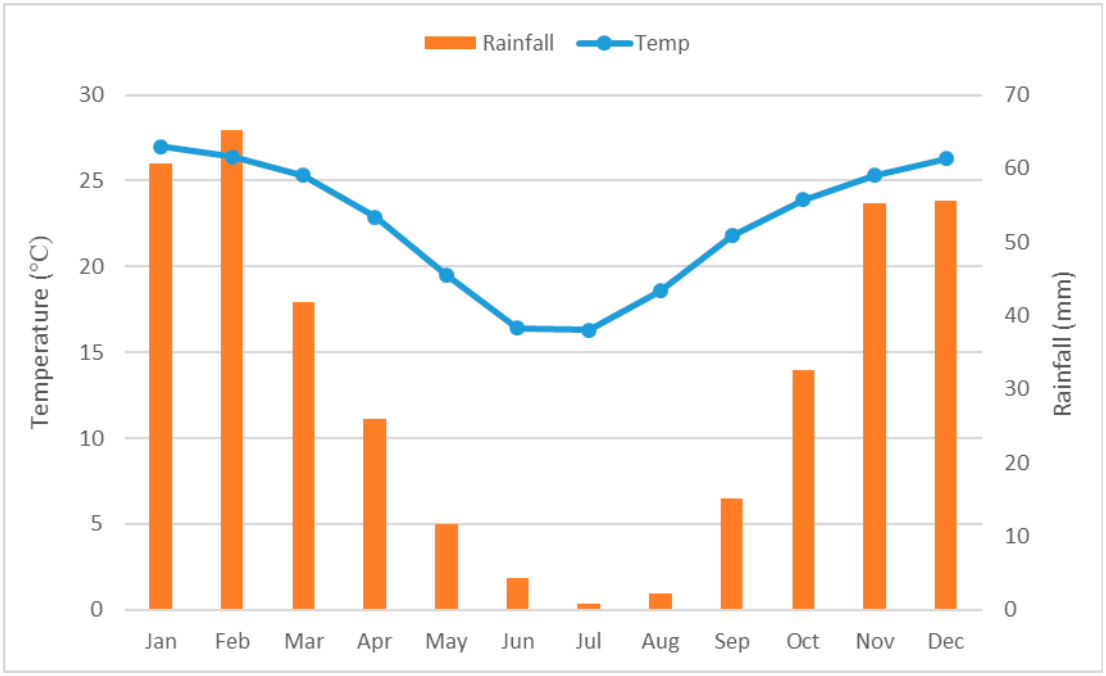

Figure 2. Average temperature and rainfall within the study areas over the past 100 years (1916–2016) (extracted from http://www.weatherbase.com).

2.2. Geology of Study Area

The study area is underlain by block-faulted Karoo Supergroup and Soutpansberg Supergroup rocks in the northern part of the Limpopo Province (Figure 3). These rocks have very low primary porosity, permeability, and storage capacity, with limited groundwater flow [24]. Mphephu geothermal spring is underlain by Wyllie's Poort and Nzhelele Formations of the Soutpansberg Supergroup. These lithologies are mainly comprised of sandstone and quartzite (Table 1). Mphephu geothermal spring is associated with the Nzhelele Fault [25].

The Sagole geothermal spring is associated with the Klein Tshipise Fault, which lies in the contact zone between Karoo and Soutpansberg Supergroups. To the south of the fault is the basalt of the Musekwa Member of the Nzhelele Formation, and to the north of the fault are the sedimentary rocks of the Madzaringwe and Mikambeni Formations of the Karoo Supergroup. The Mikambeni Formation consists of mudstone, shale, and laminated sandstone (Table 1), whereas the Madzaringwe Formation is comprised of alternating sandstone, siltstone, and shale (Table 1), with sporadically occurring coal seams [26].

The Siloam geothermal spring is found in the Nzhelele Valley at Siloam Village, which falls under the youngest formation of the Soutpansberg Group, which is the Sibasa Formation. It is dominated by basalt, which originated from the lava at the base of the formation. Basalt is responsible for the more undulating topography to the south of the Soutpansberg [27]. There are dark-red shales and sandstones that are fine, thinly-bedded sandstones. There is an interlayer of tuff, ignimbrite, and chert, and in some places, tuffaceous shale [28]. Various types of conglomerates are also available, such as argillaceous and arenaceous types. The mudstone and siltstone of Delvis Gully Member also exist [28]. Siloam Village is characterised by fractured aquifers of sandstone where groundwater occurs.

Tshipise geothermal spring is underlain by basalt and minor andesite of the Letaba Formation of Lebombo Group and Karoo Supergroup. The Lebombo Group rests on the Tshipise member of the

Clarence Formation, which is comprised of white to cream-coloured sandstones. These lithologies are intruded upon by Karoo dolerite dykes and sills with strongly developed faults [26]. The Tshipise thermal spring occurs at the intersection of two post-Permian faults in Upper Karoo, one of which is the Tshipise Fault [15].

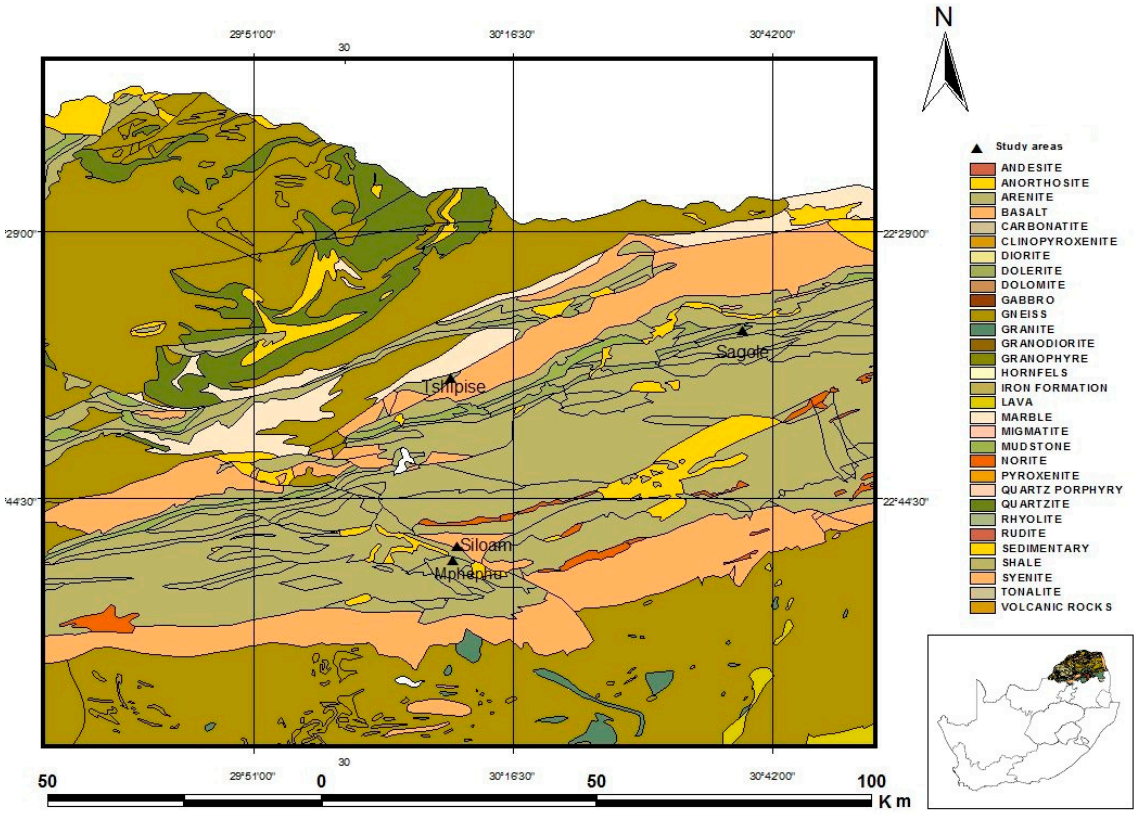

Figure 3. Geology map showing the geothermal springs within the Soutpansberg Group.

3. Materials and Methods

3.1. Sampling and Sample Pretreatment

Water samples were collected at Siloam and Tshipise geothermal springs during winter and summer seasons from October 2016–July 2017. The samples were collected thrice per season to include seasonality [29]. The geothermal water/borehole samples were collected at the source using acid-washed high-density polyethene (HDPE) containers, chilled to between 3 °C to 5 °C [30], and dispatched in a cooler box to Agricultural Research Council (ARC-ISCW) laboratory, Pretoria. The samples were allowed to cool before pre-treatment due to the high temperature of water. The HDPE containers were rinsed properly with spring water to avoid cross-contamination. Water temperatures together with other physical parameters such as pH, electrical conductivity (EC), and total dissolved solids (TDS) were measured in the field using portable multi-sensor meter (Multi 340i/SET, USA) as suggested by the American Public Health Association [31].

3.2. Analytical Methods

Samples were analysed for hydrochemical parameters in the laboratory using the standard recommended methods [31]. The sample pH, sodium absorption ratio (SAR), alkalinity, and temporary hardness were determined using ManTech Titrasip Autotitrator (Guelph, Ontario NIH6J2, Canada). The samples for anions (F^-, Cl^-, NO_3^-, SO_4^{2-}, PO_4^{3-}, HCO_3^-) and major cations (Na^+, K^+, Ca^{2+}, and Mg^{2+}) analyses were filtered and analysed using the ion chromatography method (Dionex Model DX 500) (1228 Titan way, Sunnyvale, CA 94088-3603). Quality assurance/quality control (QA/QC) was

incorporated into geothermal spring water sampling and analyses to enhance sample integrity, increase the confidence of analytical data as reliable analytical information, and prevent reporting wrong positive values caused by contamination. Field blank and splits were ensured for the water samples. The instruments used were calibrated with a standard solution to avoid analytical errors. The method detection limit (MDL) for each cation was obtained by US EPA method 200.8 [32]. The MDLs for each cation were 0.03 µg/L (Na+), 0.07 µg/L (Mg^{2+}), 0.4 µg/L (K^{+}), and 0.03 µg/L (Ca^{2+}). The MDLs for each anion were determined according to US EPA method 300.0, rev 2.1 [33] accuracy measurements methodology. The MDLs for each anion were 25 µg/L (F^{-}), 12.5 µg/L ($NO_3{}^{-}$), 500 µg/L (Cl^{-}), 125 µg/L ($SO_4{}^{2-}$), and 150 µg/L ($PO_4{}^{3-}$). The samples were analysed in triplicate to obtain the mean values of the concentrations

Stable isotopes analyses of the samples were performed using Thermo Delta V mass spectrometer connected to a Gasbench at Environmental Isotope Laboratory (EIL) iThemba LABS Johannesburg, South Africa. Samples were flushed using a mixture of either H_2 or CO_2 in He, which was also used as the equilibration gas. The water samples were equilibrated along with platinum (Pt) catalyst in preparation for deuterium measurements [34]. The equilibration time of the water samples with hydrogen gas was 40 mins, whereas carbon dioxide gas was equilibrated with water samples in about 20 h. Laboratory standards calibrated against international reference materials were analysed with each batch of the samples.

Conventionally, the isotope ratios of $^{2}H/^{1}H$ and $^{18}O/^{16}O$ in the water samples were expressed as per mil (‰) deviation relative to the Standard Mean Ocean Water (SMOW) as follows:

$$\delta\ (\%0)\ =\ \frac{R_{sampLe} - R_{smow}}{R_{smow}} \times 1000 \quad (1)$$

where R represents the ratio of heavy to light isotopes (D/H or $^{18}O/^{16}O$) in the sample and standard, respectively. The oxygen and hydrogen isotopic ratios were henceforth expressed individually as $\delta^{18}O$ and $\delta^{2}H$, respectively, or collectively as δ values. Total analytical precisions were estimated at 0.2‰ for $\delta^{18}O$ and 0.8‰ for $\delta^{2}H$. The generated Thohoyandou local meteoric water line (TLMWL) [35] was used for the interpretation of the isotopic composition of the geothermal springs.

The chloro-alkaline indices CAI 1, 2 indicate the possible ion exchange reaction between groundwater and the host environment, as suggested by Schoeller [44]. Chloro-alkaline indices used in the evaluation of base exchange were calculated using Equations (2) and (3):

$$\text{CAI-1} = \text{Cl} - (\text{Na} + \text{K})/\text{Cl} \quad (2)$$

$$\text{CAI-2} = \text{Cl} - (\text{Na} + \text{K})/(\text{SO}_4 + \text{HCO}_3 + \text{NO}_3) \quad (3)$$

All values from chemical analyses were presented as mean values and standard deviation using Microsoft Office Excel 2018. Data presentations were made using tables and graphs. Pearson's correlation coefficient was used to test the relationship between hydrochemical parameters and isotopic compositions at $\alpha = 0.05$ level of significance.

4. Results and Discussion

4.1. Physiochemical and Hydrochemical Parameters of the Geothermal Springs

The chemical composition of groundwater was not uniform but varied over a wide range. This implies that the groundwater was heterogenous in composition. Results show that geothermal spring water was more mineralised than thermal boreholes. This phenomenon supports the previous findings by Todd [36] and Olivier et al. [15]. This could be attributed to the rock-water interaction in the deeper aquifer resulting in higher mineralisation. The water temperature of springs in the study area ranged between 41.3 °C and 67.7 °C (Table 2). Based on Taylor and Phillips classification,

Siloam hot boreholes (SH1 and SH2), Mphephu, and Sagole springs are thermal (hot) waters with temperatures ranging between 41 °C to 49 °C. Siloam and Tshipise geothermal springs can be classified as scalding (hyperthermal) with temperatures ranging between 53 °C and 69 °C. There is approximately 1 °C seasonal difference in the thermal property of the geothermal spring in summer compared to winter. The high temperature in summer results in more transfer of moisture (evaporation and evapotranspiration) to the atmosphere until the dew point is reached, hence there is potential to rain more intensely in summer, resulting in more dissolution of minerals in the water. The statistical results of the hydro-chemical and isotopic analyses for the studied geothermal springs and boreholes within Soutpansberg Group are shown in Table 2.

Guidelines for Domestic Water Quality [37] delineate values of 7–9, except for Siloam geothermal spring water (SAW) and Siloam hot borehole (SH2), which had pH values of 9.39 and 9.19, respectively. The TDS values were generally less than 450 mg/l, ranging from 120.84 to 390.61 mg/l for all the samples with a slight difference with respect to seasons. Therefore, the TDS values fell within the South African Guidelines for Domestic Water Quality [37] value of 450 mg/L. However, previous studies showed that the TDS values for Tshipise geothermal spring were higher than 450 mg/L [15,18], which is contrary to the present findings. This could be a result of the decrease in water temperature (decreasing from 58 °C from Olivier et al. (2011) to 55.7 °C in the present study) of the spring and mixing of different water types.

The dominant ionic compositions found in the studied site waters were sodium (Na^+), bicarbonate (HCO_3^-), sulphate (SO_4^{2-}), and chloride (Cl^-) (Table 2). That is, the water was rich (high concentrations) in those dominant ions. The high Na+ concentrations probably originated from chemical weathering processes of sodium-rich plagioclase feldspars in the sandstone and shale. The general order of dominant cations is $Na^+ > Ca^{2+} > K^+ > Mg^{2+}$, and the sequence of the abundance of the anions are in the order: $Cl^- > SO_4^{2-} > HCO_3^- > F^- > NO_3^- > PO_4^{3-}$. The Piper and Durov diagrams were used to assess the water types and geochemical processes leading to the respective water types [38,39]. Piper diagram can classify into six fields, which are: 1) Ca-HCO_3 type; 2) Na-Cl type; 3) Ca-Mg-Cl type; 4) Ca-Na-HCO_3 type; 5.) Ca-Cl type; and 6) Na-HCO_3 type [38]. The Piper diagram revealed that most of the geothermal spring water fell in the Na-Cl water type, except the Siloam geothermal spring (SAW-WT29 and WT30) fell into the Na-HCO_3 water type (Figure 4). Although this study supports the recent findings by Durowoju et al. [18], it contradicts Olivier et al. [15], which reported $NaHCO_3$ and Na-Ca-HCO_3 water types for Sagole and Mphephu springs, respectively.

The findings from the Piper diagram were further substantiated with Durov's plot to understand the geochemical processes leading to various water types. The discrepancy in the water type could be attributed to sample size, sample preparation, and instruments used in the previous studies. Na-Cl water type was dominated by Na^+ and Cl^- derived from Na-Cl brines in winter and summer seasons, which were linked to the underlying geology emanating from gneissic rocks. Na-Cl and Na-HCO_3 water types showed a typical marine and deeper ancient groundwater influenced by ion exchange. The Na-HCO_3 water type from Siloam geothermal spring showed that the spring emanated from basalt rocks. It was the most evolved of the waters and derived their Na^+ from cation exchange of Ca^{2+} for Na^+ and K^+ as well as dissolution of rock mineral (plagioclase) [40].

The Durov diagram corroborated the findings from the Piper diagram (Figure 4). Most of the geothermal springs/groundwater aquifer were dominated by Cl and Na, and the water could result from reverse ion exchange of Na-Cl waters, consequently making the water type Na-Cl, as observed in the Piper diagram. As observed from the Piper diagram, SAW had a Na-HCO_3 water type, which was formed as a result of the reverse ion exchange of Na-Cl waters, making Cl the dominant anion and Na the dominant cation and resulting in the water Na-HCO_3 (Figure 5). Hence, the major water types were Na-Cl and Na-HCO_3, which are typical of marine and deep/deeper groundwaters influenced by ion-exchange processes, as explained earlier.

Table 2. Statistical summary of hydrochemical and isotopic compositions of studied geothermal springs.

	SAGOLE		TSHIPISE		MPHEPHU		SILOAM		
	SGW	**SGS**	**TSW**	**TSS**	**MPW**	**MPS**	**SAW**	**SH1**	**SH2**
Temp (°C)	42.4 ± 1.45	44.8 ± 2.12	54.6 ± 2.26	55.4 ± 2.21	41.3 ± 1.23	42.7 ± 1.01	67.7 ± 1.68	45.2 ± 0.00	48.4 ± 0.01
pH	8.82 ± 0.95	7.98 ± 0.22	8.46 ± 0.22	8.47 ± 0.21	8.05 ± 0.02	8.15 ± 0.07	9.39 ± 0.06	8.86 ± 0.00	9.19 ± 0.10
SAR	33.88 ± 546	19.20 ± 15.48	25.75 ± 0.98	25.45 ± 1.29	2.07 ± 0.06	2.18 ± 0.06	7.39 ± 0.04	17.25 ± 0.00	19.04 ± 0.02
EC (μS/cm)	330 ± 0.00	347.33 ± 16.17	746.67 ± 5.77	745 ± 7.07	335 ± 7.07	365 ± 21.21	340 ± 2.07	630 ± 0.00	330 ± 0.00
TDS (mg/L)	133.13 ± 1.85	196.70 ± 122.43	377.48 ± 5.36	390.61 ± 7.63	124.38 ± 1.41	120.84 ± 1.19	215.18 ± 9.25	305 ± 0.00	130.12 ± 0.00
Alkalinity (mg/L)	10.50 ± 4.24	6.50 ± 5.89	11.12 ± 0.54	10.75 ± 0.35	12.50 ± 0.00	6.00 ± 8.49	107.52 ± 1.36	10 ± 0.00	12 ± 0.00
Na (mg/L)	64.20 ± 1.84	57.13 ± 11.98	157.67 ± 4.51	154.50 ± 4.95	42.50 ± 1.27	42.35 ± 1.06	78.77 ± 7.54	118 ± 0.00	62.7 ± 0.00
K (mg/L)	1.98 ± 0.01	2.04 ± 0.05	4.55 ± 0.06	4.84 ± 0.05	2.06 ± 0.04	2.11 ± 0.01	2.61 ± 0.06	2.73 ± 0.00	2.21 ± 0.01
Ca (mg/L)	0.29 ± 0.11	4.27 ± 6.61	2.84 ± 0.07	2.79 ± 0.10	12.20 ± 0.00	11.90 ± 0.28	5.69 ± 0.05	3.53 ± 0.00	0.81 ± 0.00
Mg (mg/L)	0.00 ± 0.00	3.47 ± 6.00	0.00 ± 0.00	0.00 ± 0.00	10.50 ± 0.00	10.35 ± 0.07	1.04 ± 0.08	0 ± 0.00	0 ± 0.00
F (mg/L)	0.77 ± 0.15	2.60 ± 1.71	5.01 ± 0.63	5.98 ± 0.08	2.69 ± 0.01	4.16 ± 2.48	6.51 ± 0.08	4.55 ± 0.00	4.95 ± 0.00
NO_3 (mg/L)	0.99 ± 0.36	1.71 ± 0.85	2.13 ± 1.80	5.85 ± 1.48	3.02 ± 0.40	6.25 ± 3.23	0.60 ± 0.03	0.17 ± 0.00	1.31 ± 0.00
Cl (mg/L)	41.34 ± 0.30	81.15 ± 75.10	151.86 ± 0.28	156.67 ± 0.02	33.90 ± 0.06	98.82 ± 86.34	24.11 ± 0.77	153.3 ± 0.00	38.9 ± 0.00
SO_4 (mg/L)	16.95 ± 0.54	27.89 ± 27.23	45.81 ± 2.15	51.78 ± 0.42	9.21 ± 0.03	21.14 ± 18.31	8.99 ± 0.06	16.45 ± 0.00	10.55 ± 0.00
PO_4 (mg/L)	0.92 ± 0.82	1.30 ± 2.14	1.38 ± 1.22	2.14 ± 1.46	1.28 ± 0.74	2.26 ± 3.09	0.42 ± 0.06	1.15 ± 0.00	1.52 ± 0.00
CO_3 (mg/L)	1.50 ± 2.12	0.00 ± 0.00	0.58 ± 0.50	0.60 ± 0.42	0.00 ± 0.00	0.00 ± 0.00	16.13 ± 0.41	1.8 ± 0.00	2.4 ± 0.00
HCO_3 (mg/L)	9.76 ± 0.86	7.93 ± 7.19	12.38 ± 0.37	11.90 ± 0.43	15.25 ± 0.00	7.32 ± 10.35	98.75 ± 2.08	8.54 ± 0.00	9.76 ± 0.00
$\delta^{18}O$ (‰)	−5.82	−5.08	−5.73	−4.98	−4.92	−4.82	−5.41	−5.34	−5.25
$\delta^{2}H$ (‰)	−30.7	−30.4	−33.5	−33.2	26.1	−24.6	−27.2	−27.14	−27.46
CAI-1	−0.6	0.27	−0.07	−0.02	−0.31	0.55	−2.38	0.21	−0.67
CAI-2	−0.85	0.59	−0.17	−0.04	−0.39	1.57	−0.46	1.21	−1.08

Sample codes: TSS -Tshipise spring summer (WT01, WT03, WT05), TSW-Tshipise spring winter (WT22, WT26), SAW-Siloam geothermal spring (WT29, WT30), SH1 and SH2—Siloam hot boreholes, MPS-Mphephu spring summer (WT17, WT19), MPW-Mphephu spring winter (WT23, WT27), SGS-Sagole spring summer (WT09, WT11), SGW- Sagole spring winter (WT24, WT25, WT28).

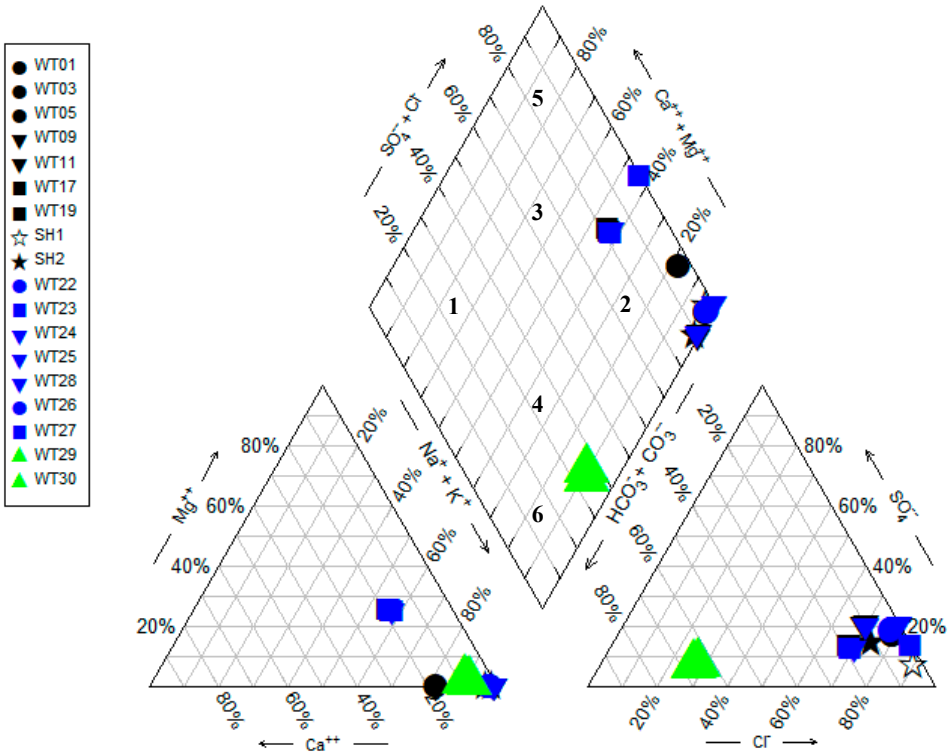

Figure 4. Piper diagram of geothermal springs within Soutpansberg Group.

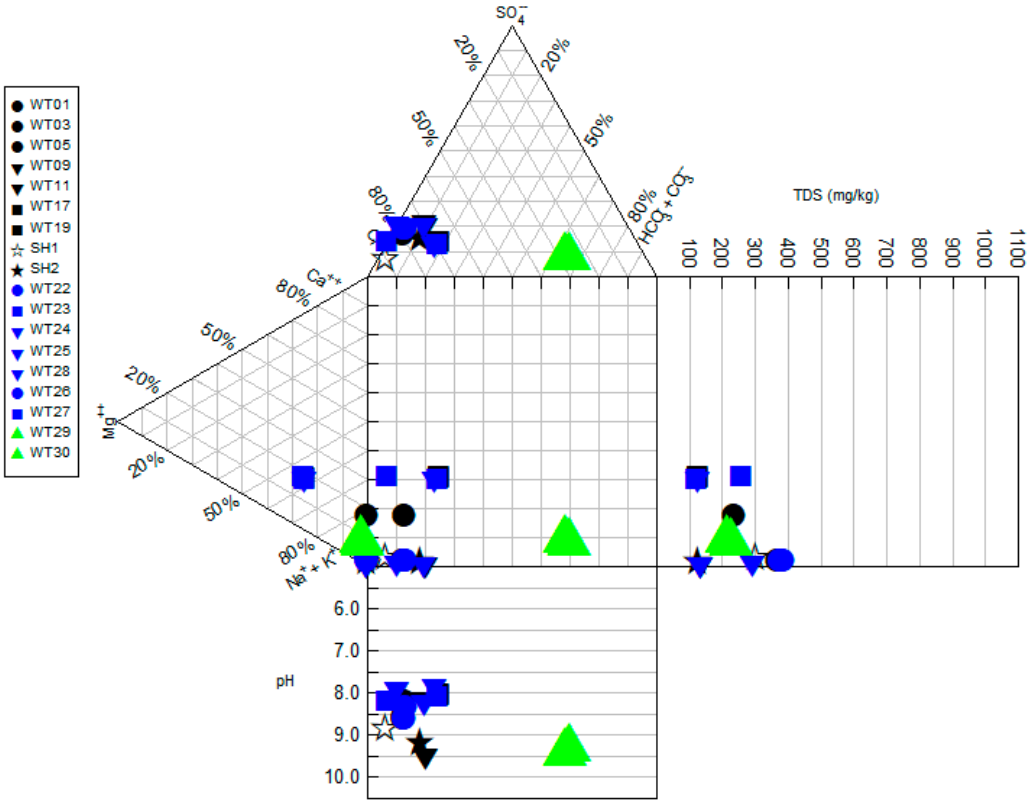

Figure 5. Durov diagram of geothermal springs within Soutpansberg Group.

There was no variation in the water type with varying seasons for the studied geothermal springs/groundwater. The Na^+ and HCO_3^- ions were also present, making the water type fall under class C (temporary hard carbonate water) [41], as reported by Olivier et al. [15]. Hence, the presence

of Na+ in groundwater in the area was due to water-rock interaction as a result of oxidisation and evapotranspiration processes. These findings supported the previous studies by Olivier et al. [15] and Durowoju et al. [18].

The processes controlling geothermal spring water/groundwater chemistry were demonstrated by Gibbs [42]. The Gibbs plot provided vital information on the mechanism (precipitation, rock-water interaction, or evaporation) controlling groundwater systems by plotting the EC against Na/(Na + Ca) and Cl/(Cl + HCO_3). Figure 6 shows all the geothermal spring water/groundwater samples in the study area plot in the rock water interaction zone, as reported by Durowoju et al. [18], for Siloam and Tshipise springs. It implied that the groundwater chemistry in the studied areas was controlled mainly by the rock-water interaction process, leading to chemical weathering of the rock-forming minerals. This implied that weathering of the aquifer material was the dominant process controlling the chemistry of the springs, resulting in the chemical budget of this water [43]. Along the path of groundwater movement from recharge to discharge areas, several chemical reactions took place with the solid phase. These chemical reactions varied temporally and spatially depending on the chemical nature of the initial water, geological formations, and residence time.

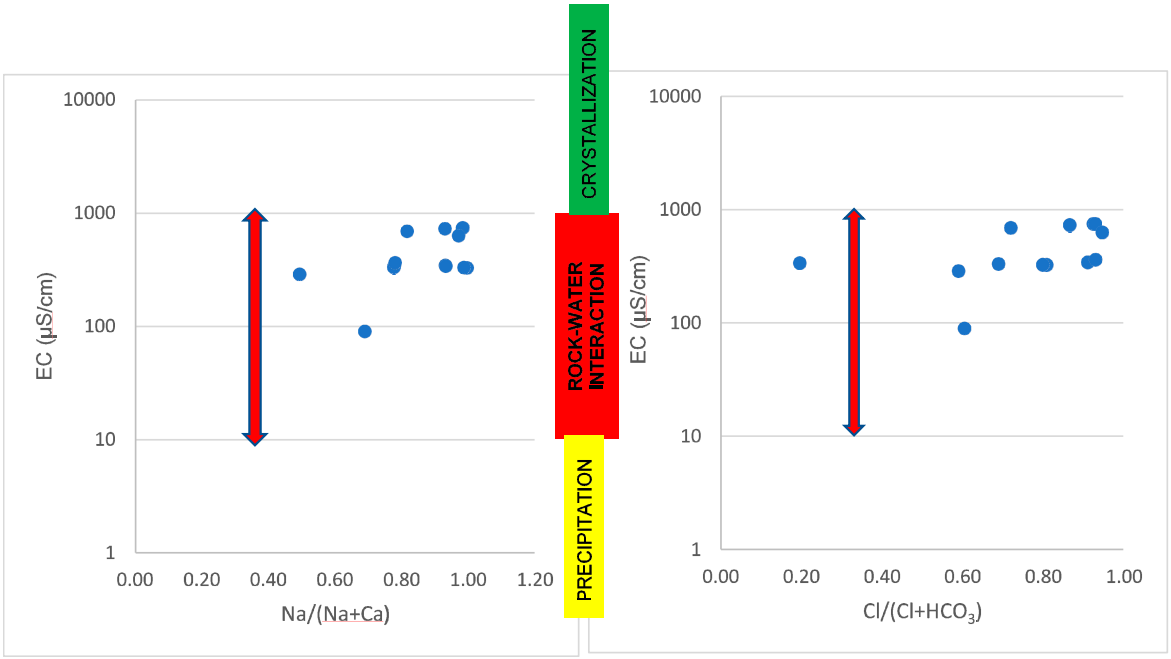

Figure 6. Mechanism controlling chemistry of the geothermal springs and other groundwaters—Gibbs plot.

In order to assess the major functional source of the dissolved solid in the groundwater, a plot of (Ca + Mg) against (HCO_3 + SO_4) was done to show the distribution of geothermal water between silicate and carbonate weathering in the system (Figure 7). The plot distinguished between carbonate and silicate weathering controlling factors. The water samples fell below and above the 1:1 line, which showed that they were in the field of silicate weathering and carbonate weathering, respectively (Figure 7). This contradicted findings from Durowoju et al. [18], which reported that Siloam and Tshipise geothermal springs fell in the silicate weathering zone. However, most of the samples fell above the 1:1 line due to the effects of the reverse ion exchange in the system (carbonate weathering), which supported the Gibb's diagram. The plotted results of Mphephu geothermal spring (MPW and MPS) fell below the 1:1 line, demonstrating the minor ion exchange process. The fact that the ions exchange processes between groundwater and the aquifer materials were relatively high was in good agreement with the Gibb's diagram.

Among chloro-alkaline indices, CAI-1 varied from (−2.38) to 0.55, and CAI-2 ranged from (−1.08) to 1.57, which were negative in the majority of the samples (67%), suggesting the presence of base-exchange process (Table 2). Ca^{2+} and Mg^{2+} exchanged Na^{+} sorbed on the exchangeable sites on the aquifer minerals, resulting in the decrease of Ca and Mg and the increase of Na in the groundwater by reverse ion exchange [44,45].

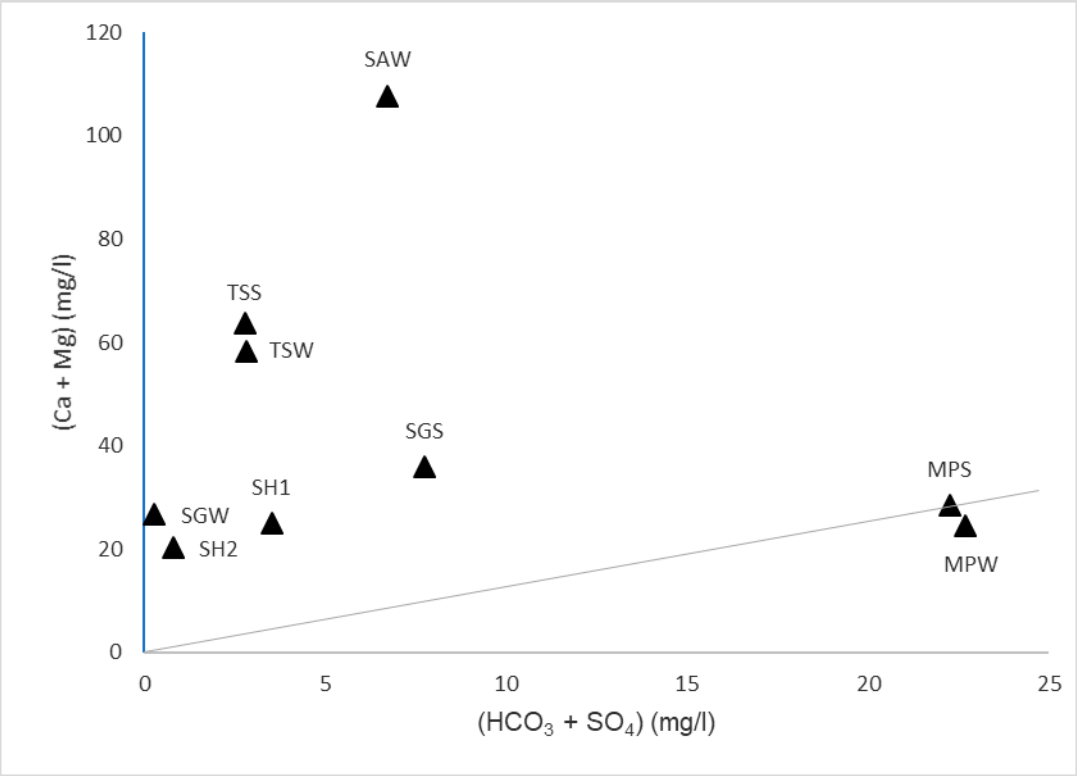

Figure 7. Relation between (Ca + Mg) and (HCO_3 + SO_4) in the geothermal springs within Soutpansberg.

This confirmed that Ca^{2+}, Mg^{2+}, and Na^{+} concentrations were interrelated through reverse ion exchange. The remaining samples were positive with direct exchange occurrence due to the direct exchange of Ca^{2+} and Mg^{2+} from the aquifer matrix with Na^{+} and K^{+} from the groundwater. This supported the fact that alkaline earth elements were abundant.

The plot of Na^{+} against Cl^{-} was used to establish the role of evaporation for higher concentrations of Na in the groundwater. Gurdak et al. [46] reported that the influence of semi-arid climate as intercalation in the soil zone enhanced active evaporation in the study area. This implied that there was loss of groundwater quantity during the summer by the action of evaporation, resulting in an increase in salt concentration in the groundwater. However, all groundwater samples plotted above the freshwater evaporation line (Figure 8). This study showed that the molar ratios of Na/Cl for the geothermal spring samples generally ranged from 0.4–3.11 compared to the seawater ratio of 0.86, which implied that 67% of the water had a Na/Cl ration higher than that of the seawater, while 33% was lower than that of seawater [9]. The weathering of silicate minerals was thus confirmed as the main source of Na in the groundwater within Soutpansberg. This indicated that evaporation was one of the processes controlling the geochemistry of the geothermal springs [46].

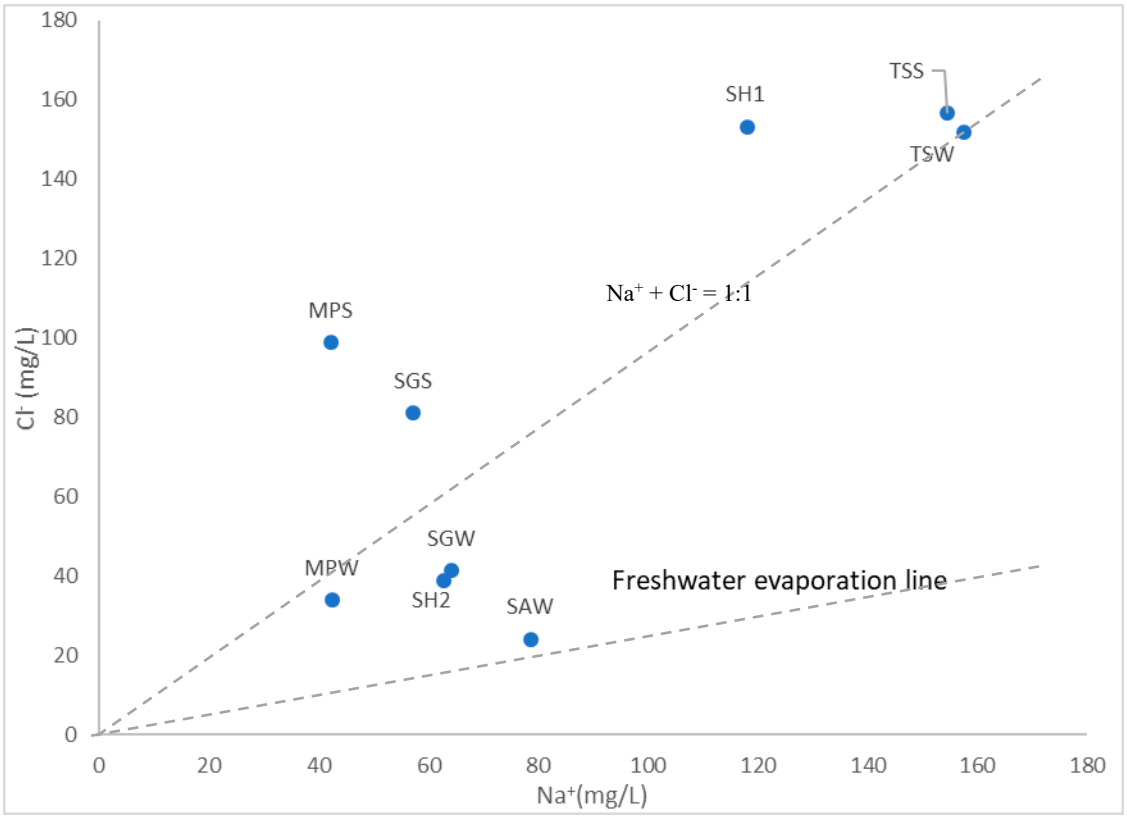

Figure 8. Relation between Na^+ and Cl^- in the geothermal springs within Soutpansberg.

4.2. Isotopic Composition

The summarised data for δ^2H and $\delta^{18}O$ values for the investigated geothermal spring water and boreholes are presented in Table 2. δ^2H and $\delta^{18}O$ values were plotted for groundwater samples, which gave us a clear understanding of the origin and recharge processes (Figure 9). It was observed that the groundwaters (geothermal springs at Tshipise, Sagole, and Mphephu) were more depleted in the winter compared to the summer season. This could be attributed to paleoclimatic effects, which make the groundwater isotopically depleted with respect to modern waters. The paleoclimatic effect is manifested by the depletion of stable isotopes with respect to modern waters [47] and is shifted along the TMWL towards negative values (Figure 9). That is to say, there is a possible evaporation of rainwater before infiltration mixing with groundwater, which would result in the slight enrichment in the summer. As mentioned earlier, most of the rainfall within Soutpansberg occurred during the summer season, but the groundwaters were more depleted in the winter than the summer season ($\delta^{18}O$ or δ^2H values were lesser). Hence, no amount effect was observed, but a high temperature effect was observed that led to evaporation, resulting in seasonal effects, which were profound in the study and supported by other studies [47–49]. The isotopic signatures of the groundwaters were depleted isotopically in the winter compared to the summer, which negated the amount effects; that is, the lesser the volume of rainfall, the higher the $\delta^{18}O$ or δ^2H content [50,51]. Figure 9 on isotopic data differentiates between the three possible types of origin of geothermal water, i.e., magnetic, oceanic, and meteoric. Ranges of $\delta^{18}O$ and δD of all the geothermal water samples are −5.7 to −4.8‰ and −33.5 to −24.6‰, respectively (Table 2). These data showed no presence of any significant amount of magnetic water, which generally has $\delta^{18}O$: +6 to +9‰ and δD: −40 to −80‰ (Pearson and Rightmire, 1980; Giggenbach, 1992). The possibility of oceanic origin of these waters was ruled out because $\delta^{18}O$ and δD were not approximately 0‰ (Craig, 1961). The isotopic compositions of groundwater (δ^2H = −24.6 to −33.5‰ and $\delta^{18}O$ = −4.82 to −5.82‰) were significantly lighter than those of modern rainwater (δ^2H = −9.8‰ and $\delta^{18}O$ = −2.7‰) [35], indicating that such groundwater could possibly originate from seepage

of meteoric water in the past during colder climates (Yeh and Lee, 2018). Hence, the origin of these waters is possibly meteoric. The isotopic ranges of the geothermal springs/groundwater were relatively reflective of rainwater signature (δD = −9.8‰ and $\delta^{18}O$ = −2.7‰). This indicated that the groundwater came from precipitation that took place in the high mountain of the Soutpansberg mountain range. Most groundwater samples might have derived from the infiltration of local precipitation with a significant contribution of another type of water in the deeper part of the aquifer.

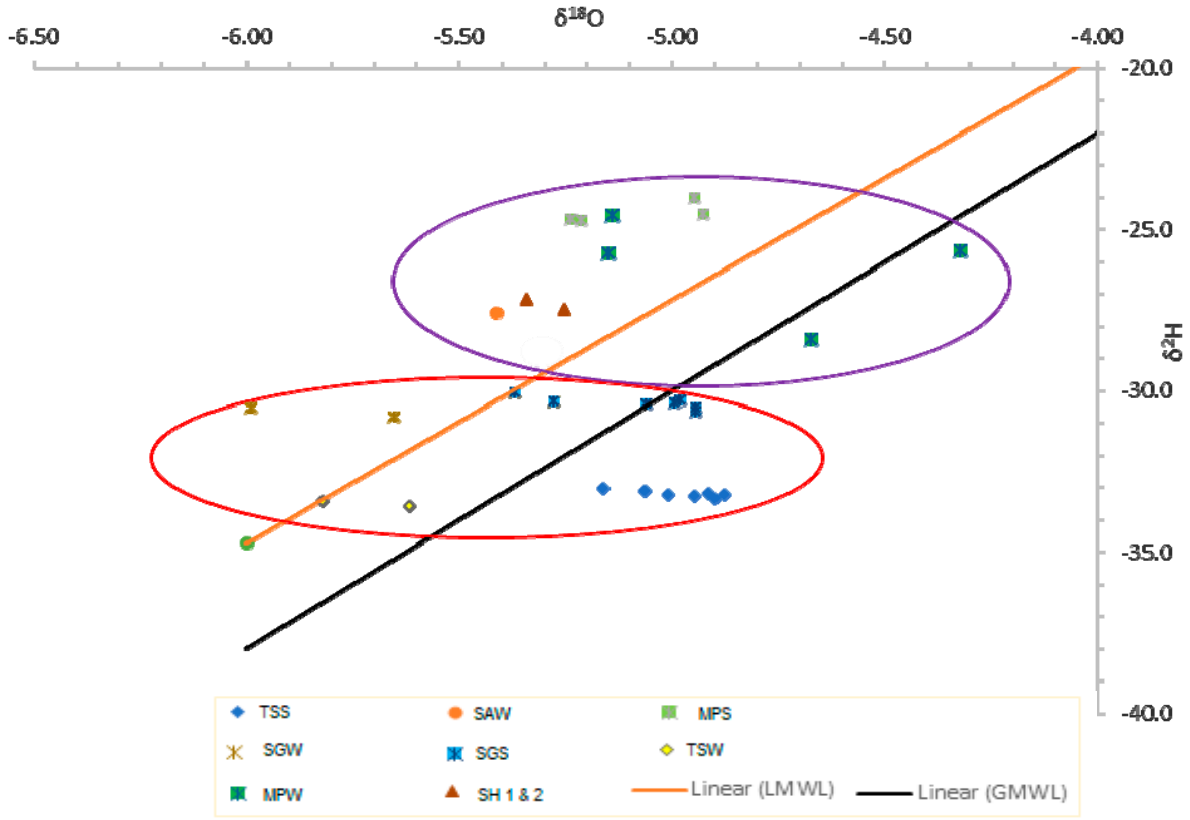

Figure 9. Seasonal variation of δ^2H and $\delta^{18}O$ values of the geothermal spring and boreholes.

The plotted δ^2H against $\delta^{18}O$ diagram shows the geothermal springs and thermal boreholes plot above/below and close to the local meteoric water line (LMWL) (Figure 9) indicative of meteoric origin, which implied that modern rainfall was the fundamental component of these groundwaters. Groundwater samples such as TSW, TSS, and SGS fell below the LMWL, which implied they were subjected to evaporation before or during their underground transit [52]. This phenomenon could have been achieved by local processes such as selective infiltration, direct percolation through the faults, degree of differentiation both on land surface and in the unsaturated (vadose) zone, and mixing mechanism from surface water and irrigation processes [9]. Other samples plotted above the LMWL, which indicated the average isotopic composition of rainwater resulting from the relatively aquifer-mixed system. This was mostly experienced in the winter with low amounts of rainfall, and this was mixed water from rainwater and other water bodies (rivers and lakes) in the aquifer. In aquifer systems that were weathered and fractured, direct infiltration through faults and shearing could have possibly conserved the isotopic composition of the original rain [9,47,52]. Hence, the groundwaters may not have been affected by isotopic differentiation, which made them distinct from rainwater resulting in the depletion of heavy isotopes due to the Rayleigh fractionation processes, which was corroborated with findings from Gat [52].

The groundwater was classified into two groups according to the isotopic composition. Sagole and Tshipise had similar signatures (Group 1), and Siloam and Mphephu had similar signatures (Group 2). This could possibly have been due to the closeness in distance above the sea level (altitude) (Siloam–835 m and Mphephu–890 m; Sagole–450 m and Tshipise–520 m) and hydraulic connectivity [53,54]. Group 1 was recharged at a higher altitude compared to Group 2, and this accounted for the slight enrichment of its isotopic compositions [47]. Also, Figure 1 shows two distinctive geological formations leading to the water chemistry of these geothermal springs, which corroborated the findings from the isotopic signatures. During the infiltration process, the water interacted with the rock minerals with depth and made the water change isotopically from depletion to enrichment (lower altitude to higher altitude). Interestingly, Siloam geothermal water and hot borehole had very similar isotopic compositions, which could be attributed either to the hydraulic connectivity between the deep and shallow aquifer that resulted from a minor fault or the fact that they were from the same aquifer. The study inferred that the geothermal spring waters were from a deep aquifer (thermal gradient) with more depleted isotopic signatures (light isotopic composition). Apparently, the thermal borehole (shallow aquifer) had a similar isotopic signature as the geothermal spring (deep aquifer), and it could be inferred that there was direct interconnectivity between the two aquifer (shallow and deep) systems through the fault at Siloam. This could be attributed to the geological formations and climatic factors of the area.

The Pearson correlation showed the relationship among physical, chemical, and isotopic compositions of the geothermal springs/boreholes (Table 3). The temperature showed a positive correlation with pH, alkalinity, K, F, CO_3, and HCO_3, and very weak negative correlation with Ca, Mg, PO_4, δ^2H, and $\delta^{18}O$. This implied that the increase in temperature increased the concentrations of the K, F, CO_3, and HCO_3, and decreased the concentrations of Ca, Mg, and PO_4, thus accounting for the high fluoride concentrations in the groundwater [2,54]. The high correlation between F^- and Na^+ was noted because it was an indication of the possible source of F^-. Dissolution of fluoride-bearing minerals, such as cryolite (Na_3AlF_6), was depicted as a source of F^- in hard rock groundwater [55]. However, further investigations are still required to deepen the existing knowledge on this issue in the studied areas. Also, the increased temperature enhanced the evaporations, leading to isotopic depletion of δ^2H and $\delta^{18}O$ in the groundwater [47–49]. Generally, δ^2H and $\delta^{18}O$ showed either strong or weak negative correlations with all the measured parameters except for Ca and Mg ($R^2 > 0.5$) (Table 3). This meant that any change in the fundamental chemistry of the water would affect the isotopic compositions of the groundwater.

Table 3. Pearson correlation matrix of correlation among physiochemical and isotopic variables in geothermal water/boreholes.

	Temp	**pH**	**SAR**	**EC**	**TDS**	**Alkalinity**	**Na**	**K**	**Ca**	**Mg**	**F**	**NO_3**	**Cl**	**SO_4**	**PO_4**	**CO_3**	**HCO_3**	**$\delta^{18}O$**	**$\delta^{2}H$**
Temp	1.00																		
pH	**0.58**	1.00																	
SAR	0.01	0.19	1.00																
EC	0.27	−0.07	0.41	1.00															
TDS	0.48	0.03	0.42	**0.95**	1.00														
Alkalinity	**0.81**	**0.62**	−0.31	−0.23	−0.01	1.00													
Na	0.47	0.15	0.52	**0.96**	**0.97**	−0.04	1.00												
K	**0.50**	0.00	0.40	**0.92**	**0.92**	−0.04	**0.94**	1.00											
Ca	−0.23	−0.54	−0.89	−0.29	−0.37	0.05	−0.47	−0.30	1.00										
Mg	−0.47	−0.65	−0.79	−0.44	−0.55	−0.17	−0.63	−0.44	**0.95**	1.00									
F	**0.79**	0.42	−0.23	0.46	**0.54**	**0.50**	**0.52**	**0.58**	−0.03	−0.27	1.00								
NO_3	−0.14	−0.57	−0.26	0.21	0.08	−0.33	0.05	0.32	0.49	**0.52**	0.16	1.00							
Cl	0.02	−0.28	0.31	**0.91**	**0.83**	−0.43	**0.79**	**0.74**	−0.16	−0.26	0.33	0.33	1.00						
SO_4	0.20	−0.36	**0.50**	**0.81**	**0.80**	−0.34	**0.78**	**0.87**	−0.27	−0.30	0.26	0.49	**0.78**	1.00					
PO_4	−0.35	−0.54	−0.07	0.32	0.13	−0.65	0.13	0.31	0.25	0.34	0.12	**0.87**	**0.51**	**0.52**	1.00				
CO_3	**0.80**	**0.72**	−0.25	−0.24	−0.02	**0.99**	−0.04	−0.07	−0.05	−0.26	**0.50**	−0.41	−0.43	−0.38	−0.67	1.00			
HCO_3	**0.81**	**0.58**	−0.33	−0.23	−0.01	**1.00**	−0.04	−0.03	0.08	−0.14	0.49	−0.31	−0.43	−0.33	−0.64	**0.98**	1.00		
$\delta^{18}O$	−0.24	−0.51	−0.68	−0.16	−0.21	−0.18	−0.34	−0.15	**0.68**	**0.69**	0.17	**0.66**	0.03	−0.03	**0.61**	−0.24	−0.16	1.00	
$\delta^{2}H$	−0.36	−0.37	−0.61	−0.35	−0.43	−0.06	−0.46	−0.35	**0.69**	**0.71**	−0.28	0.09	−0.41	−0.45	−0.07	−0.14	−0.03	0.42	1.00

Values in bold are different from 0 with a significance level alpha = 0.05.

5. Conclusions

Results of hydrochemical parameters of geothermal springs within Soutpansberg Group suggest that the thermal gradient, carbonate weathering, mineral dissolution, ion exchange, and evaporation are the main controlling geochemical processes in the variation of groundwater quality. The major water types are Na-Cl and Na-HCO_3, which are typical of marine and deep/deeper groundwaters influenced by ion-exchange processes. The δ^2H and $\delta^{18}O$ values of the geothermal spring water/boreholes confirm that the waters are of meteoric origin, which implies that rainfall is the fundamental component of these groundwaters. Thus, groundwater is derived from the infiltration of local precipitation with a significant contribution from another type of water in the deeper part of the aquifer. There is a need to further assess the surface waters around the studied geothermal springs/boreholes to ascertain groundwater and surface water interactions as well as the retention period in the aquifer. The stable isotope composition depicts that the geothermal springs at Sagole and Tshipise (Group 1) and Siloam and Mphephu (Group 2) have similar geochemical processes leading to similar isotopic compositions. Stable isotopic compositions of the geothermal spring waters/boreholes further confirm the significant role of evaporation on the groundwater chemistry of the studied areas with rock-water interaction being the main process. The isotopic signatures further confirm that there is an interconnectivity between the hot boreholes and geothermal spring at Siloam. This can be attributed to the minor faults connecting the shallow aquifer of hot boreholes to the deep aquifer of the geothermal spring. This study allowed us to significantly improve knowledge on this complex system and lay the base for considering a more rational exploitation of the geothermal spring as a resource.

Author Contributions: Conceptualisation, sampling, sample preparation and analyses were done by O.S.D.; M.B., J.O.O. and G.-I.E.E. also contributed immensely to the writing and discussion of the final manuscript. All the authors approved the final manuscript for publication.

Acknowledgments: The authors would like to thank University of Venda and Water Research Commission for funding and various forms of support. Also, the authors would like to appreciate analytical support given by Environmental Isotope Group of iThemba Laboratories, Gauteng, Johannesburg.

Conflicts of Interest: The authors declare no conflict of interest.

References

1. Kent, L.E. Thermal waters of the Union of South Africa and South West Africa. *S. Afr. J. Geol.* **1949**, *52*, 231–264.
2. Durowoju, O.S.; Odiyo, J.O.; Ekosse, G.E. Hydrogeochemical setting of geothermal springs in Limpopo Province—Review, South Africa. *Res. J. Chem. Env.* **2015**, *19*, 77–88. [CrossRef]
3. Olivier, J.; Van Niekerk, H.J.; Van Der Walt, I.J. Physical and Chemical characteristics of thermal springs in the Waterberg area of Limpopo Province, South Africa. *Water SA* **2008**, *34*, 163–174.
4. Van Vuuren, K. Die Warmwaterbronne van Suidwes-Kaapland: HulleVerbreiding, Eienskappe en Benutting. Master's Thesis, University of Stellenbosch, Stellenbosch, South Africa, 1990.
5. Lund, J.W. *Balneological Use of Thermal Water in the USA*; GHC Bulletin: Klamath Falls, OR, USA, 2000; Volume 21, pp. 31–34.
6. Gonfiantini, R. On the Isotopic Composition of Precipitation. Hydrologie et Geochimie Isotopique. In Proceedings of the International Symposium in Memory of J.-Ch. Fontes, Paris, France, 1–2 June 1995.
7. Al-Ruwaih, F.M.; Mohamed, S. Hydrochemical Processes and Environmental Isotopic Study of Groundwater in Kuwait. *Water Int.* **2004**, *29*, 158–166. [CrossRef]
8. Rajmohan, N.; Elango, L. Identification and evolution of hydrogeochemical processes in the groundwater environment in an area of the Palar and Cheyyar River Basins, Southern India. *Environ. Geol.* **2004**, *46*, 47–61. [CrossRef]
9. Ako, A.A.; Shimada, J.; Ichiyanagi, K.; Koike, K.; Hosono, T.; Eyong, G.E.T.; Iskandar, I. Isotope hydrology and hydrochemistry of water resources in the banana plain (mungo-division) of the Cameroon Volcanic line. *J. Environ. Hydrol.* **2010**, *18*, 1–20.
10. Rindl, M.R. The medicinal springs of South Africa (Supplement). *S. Afr. J. Sci.* **1916**, *13*, 528–552.

11. Rindl, M.R. The medicinal springs of South Africa (Supplement). *S. Afr. J. Sci.* **1930**, *27*, 213–226.
12. Kent, L.E. The warm springs of Loubad, near Nylstroom, Transvaal. Trans. *R. Soc. S. Afr.* **1948**, *31*, 151–168. [CrossRef]
13. Kent, L.E.; Russell, H.D. The warm spring of Buffelshoek, near Thabazimbi, Transvaal. *Trans. R. Soc. S. Afr.* **1950**, *32*, 161–175. [CrossRef]
14. Mazor, E.; Verhagen, B.T. Dissolved ions, stable and radioactive isotopes and noble gases in thermal waters of South Africa. *J. Hydrol.* **1983**, *63*, 315–329. [CrossRef]
15. Olivier, J.; Venter, J.S.; Jonker, C.Z. Thermal and Chemical Characteristics of Thermal Springs in the Northern Part of the Limpopo Province, South Africa. *Water SA* **2011**, *34*, 163–174. [CrossRef]
16. Durowoju, O.S.; Odiyo, J.O.; Ekosse, G.E. Variations of Heavy Metals from Geothermal Spring to Surrounding Soil and Mangifera Indica–Siloam Village, Limpopo Province. *Sustainability* **2016**, *8*, 60. [CrossRef]
17. Durowoju, O.S.; Odiyo, J.O.; Ekosse, G.E. Horizontal variation in trace elements and soil characteristics at Siloam and Tshipise geothermal springs, Limpopo Province, South Africa. *Water SA* **2016**, *42*, 4. [CrossRef]
18. Durowoju, O.S.; Odiyo, J.O.; Ekosse, G.E. Geochemistry of Siloam and Tshipise Geothermal Springs, Limpopo Province, South Africa. *Am. J. Environ. Sci.* **2018**. [CrossRef]
19. Makungo, R.; Odiyo, J.O.; Ndiritu, J.G.; Mwaka, B. Rainfall-runoff modelling approach for ungauged catchments: A case study of Nzhelele River sub-quaternary catchment. *Phys. Chem. Earth* **2010**, *35*, 596–607. [CrossRef]
20. Kent, L.E. The thermal waters in the Republic of South Africa. In Proceedings of the Symposium II on Mineral and Thermal Waters of the World, B—Overseas Countries, Academia, Prague, Czech Republic, 1969; Volume 19, pp. 143–164.
21. Kottek, M.; Grieser, J.; Beck, C.; Rudolf, B.; Rubel, R. World Map of the Köppen-Geiger climate classification updated. *Meteorol. Z.* **2006**, *15*, 259–263. [CrossRef]
22. Makungo, T.E. The Adequacy of Water Supply to Meet the Demand in Siloam Village of Limpopo Province of South Africa. Bachelor's Thesis, University of Venda, Thohoyandou, South Africa, 2008.
23. Department of Water Affairs and Forestry (DWAF). *Luvuvhu/Letaba Water Management Area: Water Resource Situation Assessment*; Report NO P0200/00/030/; WSM (pty) Ltd.: Pretoria, South Africa, 2001.
24. Brandl, G.; Soutpansberg Group. *Catalogue of South Africa Lithostratigraphic Units*; Council for Geoscience: Pretoria, South Africa, 1999; pp. 6–41.
25. Brandl, G.; Council for Geoscience. *The Geology of the Alldays Area: Explanation: Sheet 2228*; Council for Geoscience: Pretoria, South Africa, 2002; p. 71.
26. Johnson, M.R.; Anhaeusser, C.R.; Thomas, R.J. *The geology of South Africa*; Geological Society of South Africa: Johannesburg, South Africa; Council for Geosciences: Pretoria, South Africa, 2006; pp. 301–318.
27. Brandl, G.; Geological Survey. *The Geology of the Pietersburg Area: Explanation of Sheet 2328*; Government Printer: Pietersburg, South Africa, 1986; p. 43.
28. Mundalamo, H.R. Investigation of Water Quality in Nzhelele Valley, Limpopo Province, South Africa. Bachelor's Thesis, University of Venda, Thohoyandou, South Africa, 2003.
29. United States Environmental Protection Agency (USEPA). *Guideline for Water Reuse*; EPA/625/R-04/108; EPA: Washington, DC, USA, 2004.
30. APHA. *Standard Methods for the Examination of Water and Wastewater*, 20th ed.; American Public Health Association: Washington DC, USA, 1998.
31. United State Environmental Protection Agency (USEPA). Method 200.8. Determination of Trace Elements in Waters and Wastes by ICP, Revision 5.4. 1994. Available online: http://www.epa.gov/sam/pdfs/EPA-200.8.pdf (accessed on 11 November 2017).
32. United State Environmental Protection Agency (USEPA). *Determination of Inorganic Anion in Water by Ion Chromatography*; Method 300.0. Rev 2.1; US Environmental Agency: Cincinnati, OH, USA, 1993.
33. Dolnikowski, G.G. A New Sample Preparation Method for Isotope Ratio Mass Spectrometry of 2H-Enriched Samples Generated by the Doubly Labeled Water Method. *Obesity* **1955**. [CrossRef]
34. Durowoju, O.S.; Odiyo, J.O.; Ekosse, G.E. Determination of isotopic composition of rainwater to generate local meteoric water line in Thohoyandou, Limpopo Province, South Africa. *Water SA* **2019**, accepted.
35. Todd, D.K. *Groundwater Hydrology*, 2nd ed.; John Wiley: New York, NY, USA; Chichester, UK; Brisbane, Australia; Toronto, ON, Canada, 1980; ISBN 0 471 87616X.

36. Department of Water Affairs and Forestry (DWAF). *South African Water Quality Guidelines, Volume 1: Domestic Water Use*, 2nd ed.; DWAF: Pretoria, South Africa, 1996.
37. Piper, A.M. A graphic procedure in geochemical interpretation of water analyses. *Trans. Am. Geophys. Union* **1944**, *25*, 914–923. [CrossRef]
38. Durov, S.A. Classification of natural waters and graphical representation of their composition. *Dokl. Akad. Nauk. USSR* **1948**, *59*, 87–90.
39. Yahaya, M.I.; Mohammad, S.; Abdullahi, B.K. Seasonal variations of heavy metals concentrations in Abattoir dumping site soil in Nigeria. *J. Appl. Sci. Environ. Manag.* **2009**, *13*, 9–13. [CrossRef]
40. Lipfert, G.; Reeve, A.S.; Sidle, W.; Marvinney, R. Geochemical patterns in an arsenic-tainted, fracture—Bedrock groundwater system in Northport, Maine USA. *Appl. Geochem.* **2006**, *26*, 747–762.
41. Bond, G.W. A geochemical survey of the underground water supplies of the Union of South Africa. *Memoirs Geol. Surv. S. Afr.* **1946**, *41*, 208.
42. Gibbs, R.J. Mechanisms controlling world water chemistry. *Science* **1970**, *170*, 1088–1090. [CrossRef]
43. Aghazadeh, N.; Mogaddam, A.A. Assessment of groundwater quality and its suitability for drinking and agricultural uses in the Oshnavieh area, Northwest of Iran. *J. Environ. Prot.* **2010**, *1*, 30–40. [CrossRef]
44. Schoeller, H. Geochemistry of groundwater. In *Groundwater Studies—An international Guide for Research and Practice*; UNESCO: Paris, France, 1977; pp. 1–18.
45. Glover, E.T.; Akiti, T.T.; Osae, S. Major ion chemistry and identification of hydrogeochemical processes of groundwater in Accra Plains. *Geoscience* **2012**, *50*, 10279–10288.
46. Gurdak, J.J.; Hanson, R.T.; McMahon, P.B.; Bruce, B.W.; McCray, J.E.; Thyne, G.D.; Reedy, R.C. Climate variability controls on unsaturated water and chemical movement, High Plans Aquifer, USA. *Vadose Zone J.* **2007**, *6*, 533–547. [CrossRef]
47. Kebede, S. *Groundwater in Ethiopia*; Springer: Berlin/Heidelberg, Germany, 2013; pp. 187–203.
48. Gat, J.R.; Gonfiantini, R. *Stable Isotope Hydrology: Dueterium and Oxygen-18 in the Water Cycle*; International Atomic Energy Agency: Vienna, Austria, 1981.
49. Kebede, S.; Travi, Y. Origin of the $\delta^{18}O$ and $\delta^{2}H$ composition of meteoric waters in Ethiopia. *Quart. Int.* **2012**, *257*, 4–12. [CrossRef]
50. Dansgaard, W. Stable isotopes in precipitation. *Tellus* **1964**, *16*, 436–468. [CrossRef]
51. Coplen, T.B.; Herczeg, A.L.; Barnes, C. Isotope engineering-using stable isotopes of water molecule to solve practical problems. In *Environmental Tracers in Catchment Hydrology*; Cook, P., Herczeg, A.L., Eds.; Kluwer Academic Publishers: Norwell, MA, USA, 2000; pp. 79–110.
52. Gat, J.R. *Isotope Hydrology: A Study of the Water Cycle*; Series on Environmental Science and Management; Imperial College Press: London, UK, 2010.
53. Edmunds, W.M.; Fellman, E.; Goni, I.B.; Prudhomme, C. Spatial temporal distribution of groundwater recharge in northern Nigeria. *Hydrogeol. J.* **2002**, *10*, 205–215. [CrossRef]
54. Fantong, W.Y.; Satake, H.; Ayonghe, S.N.; Aka, F.T.; Kasuyoshi, A. Hydrogeochemical controls and usability of groundwater in the semi-arid Mayo Tsanaga River Basin: Far north province, Cameroon. *J. Environ. Earth Sci.* **2008**. [CrossRef]
55. Odiyo, J.O.; Makungo, R. Fluoride concentrations in groundwater and impact on human health in Siloam Village, Limpopo Province, South Africa. *Water SA* **2012**, *38*, 731–736. [CrossRef]
56. Mahamat, H.B.; Coz, M.L.; Abderamane, H.; Sardini, P.; Razack, M. Hydrochemical and Isotopic Characteristics of the Basement Aquifer in the Wadi Fira Area, Eastern Chad. *J. Water Resour. Prot.* **2017**, *9*, 1688–1708. [CrossRef]